

Bioactive Peptides/Chitosan Nanoparticles Enhance Cellular Antioxidant Activity of (–)-Epigallocatechin-3-gallate

Bing Hu,^{†,‡} Yuwen Ting,[‡] Xiaoxiong Zeng,^{*,†} and Qingrong Huang^{*,‡}

[†]College of Food Science and Technology, Nanjing Agricultural University, Nanjing 210095, People's Republic of China

[‡]Department of Food Science, Rutgers University, New Brunswick, New Jersey 08901, United States

ABSTRACT: (–)-Epigallocatechin-3-gallate (EGCG), one representative of the well-studied chemopreventive phytochemicals but with low bioavailability, was encapsulated in monodispersed nanoparticles that were assembled from bioactive caseinophosphopeptide (CPP) and chitosan (CS). The encapsulation efficiency of EGCG in CS–CPP nanoparticles ranged from 70.5 to 81.7%; meanwhile, the *in vitro* release of EGCG from CS–CPP nanoparticles was in a controllable manner. The EGCG-loaded CS–CPP nanoparticles exerted stronger activity of scavenging free radical than the free EGCG ($p < 0.01$) in the cellular antioxidant activity assay. Furthermore, cellular uptake of the EGCG-loaded CS–CPP nanoparticles was confirmed by the green fluorescence inside the human hepatocellular carcinoma (HepG2) cells, which was considered to play an important role in the improvement of the antioxidant activity of the nanoencapsulated EGCG. The results suggested that encapsulation of EGCG using CS–CPP nanoparticles should be a potential approach to enhance its antioxidant activity in biological systems.

KEYWORDS: EGCG, caseinophosphopeptide, chitosan, nanoparticle, cellular antioxidant activity, cellular uptake

■ INTRODUCTION

Free radicals and oxidative stress are related to cancer, cardiovascular disease, diabetes, autoimmune disorders, and neurological disorders.¹ There is accumulating evidence from population as well as laboratory studies to support an inverse relationship between regular consumption of diets enriched in antioxidants and the risk of such disorders. (–)-Epigallocatechin-3-gallate (EGCG), the most abundant of tea catechins in green tea, is known as a strong natural antioxidant in our diet. A lot of epidemiological and preclinical studies have demonstrated that EGCG can reduce the risk of cancer as well as cardiovascular, neurodegenerative, and other diseases.² Drug discovery screening results suggest that EGCG is a promising new drug candidate because it is the most potent inhibitor of protein kinase C among the tested natural compounds and their derivatives.³ Furthermore, there is considerable evidence that EGCG can inhibit enzyme activities and signal transduction pathways, resulting in the suppression of cell proliferation and enhancement of apoptosis, as well as the inhibition of cell invasion, angiogenesis, and metastasis.⁴ Oral administration is considered as the most efficient delivery system of antioxidants; however, oral bioavailability of EGCG is quite low,⁵ which is mainly attributed to its poor stability and intestinal absorption.⁶ As a consequence, only a relatively small amount of EGCG can enter the bloodstream and further reach the targeted sites.

Development of nanostructured biomaterials for encapsulation of phytochemicals is of special interest from pharmaceutical and functional food points of view, to overcome their limitation and enhance the bioavailability of the corresponding phytochemicals, so that the goal of nanochemoprevention can be achieved.^{7–10} However, the nanocarriers used currently are usually non-natural products, which are more suitable for parenteral injections rather than oral consumption.^{11–13} In our previous study, pioneering research to improve nanochemo-

prevention of EGCG by oral consumption through encapsulation with food-grade nanoparticles of chitosan–caseinophosphopeptide (CS–CPP) has been achieved. These CS–CPP nanostructures are highly biocompatible and able to enhance the intestinal absorption of EGCG across the *in vitro* Caco-2 cell monolayers significantly.^{14–16}

The biological and pharmacological effects of EGCG may be primarily associated with its antioxidant activity, and many studies are therefore focused on evaluation of the antioxidant activity of EGCG after encapsulation with different nanostructures. Li et al. reported that the antioxidant activity of EGCG can be preserved after encapsulation with heat-treated β -lactoglobulin nanoparticles to reduce ferric iron and 2,2-diphenylpicrylhydrazyl (DPPH), respectively.¹⁷ Peres et al. found that carbohydrate nanoparticles composed of gum arabic and maltodextrin are able to prevent EGCG radical scavenging capacity using the DPPH assay.¹⁸ In addition, the antioxidant activity of CS–tripolyphosphate (CS–TPP) nanoparticles encapsulated or chemically grafted with polyphenol compounds was also determined by the DPPH assay, ferric-reducing antioxidant power (FRAP) assay, and β -carotene bleaching assay.^{19,20} However, none of these assays took into account the bioavailability, uptake, and metabolism of the nanoparticle-loaded antioxidant compounds. Biological systems are much more complex than the simple chemical mixtures employed, and it is hard to predict their activity *in vivo* by using these chemical antioxidant activity assays.

Cell culture models provide an approach that is relatively fast and cost-effective and addresses certain issues of uptake, distribution, and metabolism. The cellular antioxidant activity

Received: November 13, 2012

Revised: December 27, 2012

Accepted: January 7, 2013

Published: January 8, 2013

(CAA) assay is a cell-based method for determining the antioxidant activity of phytochemicals.²¹ Recently, it has been introduced to measure the antioxidant activity of micelle-encapsulated curcuminoids²² and nanoemulsion-loaded resveratrol.²³ Direct cellular uptake of nanostructures is usually predicted to play an essential role in the elevation of cellular antioxidant activities of phytochemicals after nanoencapsulation with micelle and nanoemulsions, which, however, still need to be further confirmed by experiments.

Herein, we report the use of CS–CPP nanoparticles as effective nanocarriers for enhancing the CAA of EGCG. The morphology and particle size of CS–CPP nanoparticles loaded with EGCG were observed and determined by atomic force microscopy (AFM). The particle size and surface charge of the nanoparticles were characterized using dynamic light scattering (DLS) and electrophoretic mobility (ζ potential) measurements. The encapsulation efficiency and *in vitro* release profile of EGCG from the nanoparticles were determined by centrifugation combined with high-performance liquid chromatography (HPLC). The antioxidant activity of nano-encapsulated EGCG as well as free EGCG was determined by the CAA assay. The cellular uptake fate of the fluorescently labeled CS–CPP nanoparticles was investigated via fluorescence microscopy. Finally, the mechanism underlying the elevation of EGCG CAA after delivery by CS–CPP nanoparticles was illustrated.

MATERIALS AND METHODS

Materials. CPP was prepared and identified by high-performance liquid chromatography–tandem mass spectrometry (HPLC–MS/MS) according to our reported methods.¹⁴ The human hepatocellular carcinoma (HepG2) cell line was a gift from Dr. Mou-Tuan Huang (Rutgers, The State University of New Jersey, New Brunswick, NJ). CS with a molecular weight of 100 kDa (derived from crab shell, with a degree of deacetylation of 90%) was obtained from Golden-Shell Biochemical Co., Ltd. (Hangzhou, China). EGCG, 2',7'-dichloro-fluorescein diacetate (DCFH-DA), Dulbecco's modified Eagle's medium (DMEM), trypan blue, and paraformaldehyde were purchased from Sigma-Aldrich Co. (St. Louis, MO). HPLC-grade acetonitrile (MeCN), 100× penicillin and streptomycin, 0.25% trypsin with ethylenediaminetetraacetic acid (EDTA), acetic acid, and 1 M 4-(2-hydroxyethyl)-1-piperazineethanesulfonic acid (HEPES) were purchased from Fisher Scientific (Pittsburgh, PA). 2,2'-Azobis(2-amidinopropane) dihydrochloride (ABAP) was purchased from Wako Chemicals (Richmond, VA). Sodium carbonate and methanol were obtained from Mallinckrodt Baker (Phillipsburg, NJ). Williams' medium E (WME) and Hank balanced salt solution (HBSS) were purchased from HyClone Laboratories (Logan, UT). Fetal bovine serum (FBS) was obtained from Atlanta Biologicals (Lawrenceville, GA). All other reagents were of analytical grade.

General Procedure for the Preparation of Nanoparticles. CS–CPP nanoparticles were prepared according to our reported method,¹⁴ with minor modification. Briefly, 50 mg of CS was dissolved in 1.0% (w/v) acetic acid solution with sonication until the solution was transparent. The aqueous solution of CPP was obtained at a suitable concentration. Both CS and CPP solution were adjusted to pH 6.2 with 1.0 N HCl or NaOH solution. By consequential addition of CS solution to the CPP solution with stirring at room temperature, the formation of CS–CPP nanoparticles started spontaneously via the CPP-initiated ionic gelation mechanism. For the preparation of EGCG-loaded CS–CPP nanoparticles, aqueous solution of EGCG was added to CPP solution before the addition of CS solution. The nanoparticle suspensions were immediately subjected to further analysis and application.

Characterization of EGCG-Loaded CS–CPP Nanoparticles. The mean particle size and size distribution were determined using a DLS-based BIC 90 plus particle size analyzer (Brookhaven Instrument

Co., Holtsville, NY) at a fixed scattering angle of 90° at 25 ± 1 °C. Electrophoretic mobility (a particle's velocity in an electric field) for homogeneous and mixed CS–CPP systems was investigated using a Zetasizer Nano ZS90 (Malvern Instruments, Westborough, MA). All measurements were run in triplicate. Morphological evaluation of the nanoparticles was performed by AFM. All AFM images were recorded with a Digital Instruments Nanoscope IIIA multimode in tapping mode using a silicon tip with nominal spring constant of 40 N/m at room temperature.

Evaluation of Encapsulation Efficiency and *in Vitro* Release of EGCG. The encapsulation efficiency of EGCG in CS–CPP nanoparticles was determined according to our reported method,²⁴ with minor modification. Briefly, EGCG-loaded CS–CPP nanoparticles were carefully transferred to the filter unit of an Amicon Ultra-15 centrifugal filter device (Millipore Co., Billerica, MA) with a low-binding Ultracel membrane [molecular weight cut-off (MWCO) of 1000]. After centrifugation at 4000g for 45 min, the amount of EGCG in ultrafiltrate was determined by HPLC according to our reported method.²⁵ The EGCG-loaded CS–CPP nanoparticles in the filter unit were freeze-dried by a Labconco freeze-dry system (Labconco Co., Kansas City, MO). The encapsulation efficiency of EGCG was calculated using the formula

$$\text{encapsulation efficiency (\%)} = \left(\frac{\text{total amount of EGCG} - \text{amount of EGCG in ultrafiltrate}}{\text{total amount of EGCG}} \right) \times 100$$

The EGCG-loaded CS–CPP nanoparticles obtained from the centrifugation were further used to determine the *in vitro* release profile of EGCG. First, nanoparticles in the filter unit were diluted by 0.01 M phosphate-buffered saline (PBS) (pH 6.2) to 2.0 mL. Then, the filter unit was sealed and placed in a water bath of 37 °C. At a specified collection time, the filter unit was placed back into the Amicon Ultra-15 centrifugal filter device and centrifuged at 4000g for 45 min. The nanoparticles in the filter unit were treated repeatedly, as described above. The amount of EGCG in each ultrafiltrate was determined by HPLC, and the total released EGCG mass M_i at time i was calculated using the formula

$$M_i = C_i V_i + \sum C_{i-1} V_{i-1}$$

where C_i is the concentration of EGCG in the ultrafiltrate at time i and V_i is the ultrafiltrate volume.

Determination of CAA of Nanoparticle-Encapsulated EGCG and Free EGCG. A CAA assay was performed as the reported procedure,²¹ with small modifications. Briefly, HepG2 cells were grown in minimum essential medium (MEM) growth medium supplemented with 10% FBS, 10 mM HEPES, 100 units/mL penicillin, and 100 µg/mL streptomycin in a humidified atmosphere with 5% CO₂ at 37 °C. The cells used in the present study were between passages 8 and 20. HepG2 cells at a density of 6 × 10⁴/well were seeded in a 96-well plate (100 µL/well). After 24 h of incubation, the WME growth medium was removed and the wells were washed with PBS. Triplicate wells were treated for 1 h with 100 µL of EGCG solution or EGCG-loaded CS–CPP nanoparticles plus 25 µM DCFH-DA dissolved in treatment medium. After 1 h, the wells were washed with 100 µL of PBS. Then, 600 µM ABAP was applied to the cells in 100 µL of HBSS, and the 96-well microplate was placed into a Fluoroskan Ascent FL plate-reader at 37 °C. Emission at 538 nm was measured with excitation at 485 nm every 5 min for 1 h. Each plate included triplicate control (containing cells treated with DCFH-DA and HBSS with ABAP) and blank (containing cells treated with DCFH-DA and HBSS without ABAP) wells. For the EGCG-loaded CS–CPP nanoparticles, the neat CS–CPP nanoparticles without EGCG were also used as the blank. After blank subtraction from the fluorescence readings, the area under the curve of fluorescence versus time was integrated to calculate the CAA value at each concentration of EGCG or EGCG-loaded CS–CPP nanoparticles as follows:

$$\text{CAA value} = 100 - \left(\frac{\int \text{SA}}{\int \text{CA}} \right) \times 100$$

where $\int \text{SA}$ is the integrated area under the sample fluorescence versus time curve and $\int \text{CA}$ is the integrated area from the control curve. The median effective dose (EC_{50}) was determined for EGCG or EGCG-loaded CS–CPP nanoparticles from the median effect plot of $\log(\text{fa}/\text{fu})$ versus $\log(\text{dose})$, where fa is the fraction affected and fu is the fraction unaffected by the treatment.

Cellular Uptake of Nanoparticles. The cellular uptake of nanoparticles by HepG2 cells was studied according to reported methods,^{16,26} with small modifications. First, CS was labeled with fluorescein isothiocyanate (FITC). HepG2 cells between passages 8 and 20 were seeded into Lab-Tek chambered coverglasses (Thermo Scientific Nunc, Thermo Scientific) at a density of 5×10^4 cells/cm² and cultured in 0.6 mL of MEM growth medium in a humidified atmosphere with 5% CO₂ at 37 °C. After 2 days of culture, the cell monolayers were washed twice and preincubated with 0.6 mL of prewarmed transport medium (pH 6.2) for 30 min at 37 °C. Uptake was initiated by the addition of 0.6 mL of EGCG-loaded FITC-labeled CS–CPP nanoparticles (FNPE) or FITC-labeled CS (FCS) solution diluted by the medium to a final CS concentration of 0.125 mg/mL. After 2 h of incubation at 37 °C, FNPE or FCS was removed and the cells were washed twice with prewarmed PBS solution and fixed in 4% paraformaldehyde for 10 min. The specimens after storage overnight at 4 °C in cell freezing medium, serum-free (Sigma-Aldrich, St. Louis, MO) were examined under a fluorescence microscope. The fluorescence micrographs were recorded with a Nikon TE-2000-U inverted fluorescence microscope equipped with a charge-coupled device (CCD) camera (Retiga EXi, QImaging). Images were taken at the same region under visible light and bandpass filter to observe the fluorescence signals emitting from FNPE or FCS (excitation at 488 ± 10 nm and emission at 520 ± 10 nm). All images were processed by SimplePCI C-Imaging software (Compix, Inc., Sewickley, PA).

Statistical Analysis. The experiments and analyses were performed at least in triplicate. Data were expressed as means \pm standard deviation (SD). The antioxidant activities of free and encapsulated EGCG in CS–CPP nanoparticles were compared by one-way analysis of variance (ANOVA) with *t* test using SigmaPlot 10.0 software (Systat Software, Inc., Chicago, IL). A *p* < 0.01 value was considered to be statistically significant.

RESULTS

Characterization of EGCG-Loaded CS–CPP Nanoparticles. The morphology of the EGCG-loaded CS–CPP nanoparticles was observed by tapping-mode AFM in the scan size of $20 \times 20 \mu\text{m}$. As depicted in Figure 1, the nanoparticles were sphere-like and dispersed homogeneously. In AFM images, the particle size can be determined through measuring the vertical distance of the nanoparticle in height mode using the section analysis, as depicted in Figure 2, which was taken in a much smaller scan size of $5 \times 5 \mu\text{m}$ to make the measurement result more accurate. The vertical distance of the selected nanoparticle in Figure 2 was 69.2 nm. By averaging the vertical distances of nanoparticles in the height mode using the section analysis, the mean apparent particle diameter of the nanoparticles was 74.5 nm. As a comparison, we determined the mean hydrodynamic diameter of the EGCG-loaded CS–CPP nanoparticles by means of the DLS method. The particle size determined by DLS at room temperature was 143.7 ± 6.7 nm ($n = 3$), with the polydispersity index ranging from 0.08 to 0.13, which indicated that a homogeneous dispersion of nanoparticles was obtained. Notably, the particle size measured from the AFM image was much smaller than that from DLS, which was mainly due to the process involved in the preparation of the samples. It is known that AFM gives images of the particles in the dry state, while DLS depicts the value of the particle size

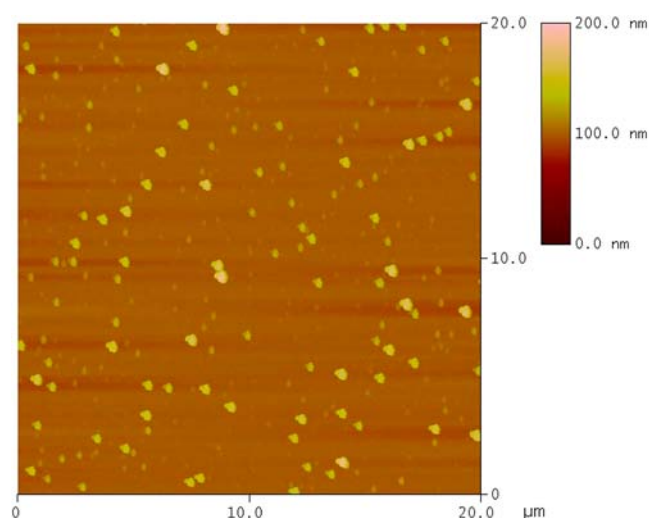


Figure 1. Surface morphology image of the EGCG-loaded CS–CPP nanoparticles at pH 6.2 (CS/CPP mass ratio, 2:3; EGCG/CPP mass ratio, 1:2).

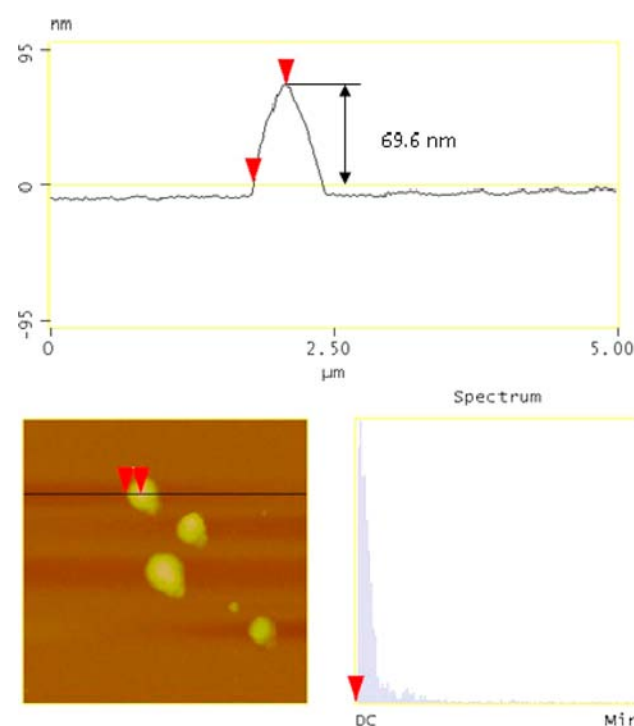


Figure 2. Section analysis of the EGCG-loaded CS–CPP nanoparticles in the height mode of an AFM image.

in solution of the sample. As a type of hydrogel, the CS–CPP nanoparticles in solution were in the swollen state and could take up large amounts of water. Therefore, the size determined by DLS included hydrated layers surrounding the nanoparticles, and it was much larger than that in the dry state determined by AFM. Similar results have been reported in previous studies.^{27,28} The surface charge of the EGCG-loaded CS–CPP nanoparticles was 30.8 ± 4.6 mV.

Encapsulation Efficiency and *in Vitro* Release of EGCG.

In the present study, we found that the encapsulation efficiency increased from 70.5 to 81.7% with the increase of the EGCG concentration from 1.0 to 2.5 mg/mL (Table 1), which is consistent with our previous results of the quartz crystal

Table 1. Encapsulation Efficiency of EGCG in CS–CPP Nanoparticles with Different Initial EGCG Concentrations at a CS/CPP Mass Ratio = 2:3

concentration of EGCG (mg/mL)	1	1.5	2.5
encapsulation efficiency (%)	70.5 ± 3.0	75.9 ± 3.2	81.7 ± 4.1

microbalance with dissipation monitoring (QCMD).¹⁵ Furthermore, in correspondence with the encapsulation efficiency, the *in vitro* release profile of EGCG showed that both the release kinetics and total release amount of EGCG at isothermal conditions (37 °C) increased as the initial concentration of EGCG increased from 1.0 to 2.5 mg/mL (Figure 3). At the beginning 12 h, EGCG was released quickly

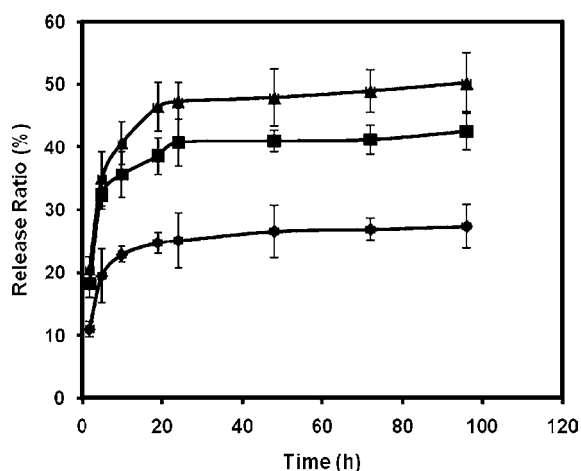


Figure 3. Effect of EGCG concentrations (◆, 1.0 mg/mL; ■, 1.5 mg/mL; ▲, 2.5 mg/mL) on *in vitro* release profiles of EGCG from CS–CPP nanoparticles (CS/CPP mass ratio, 2:3; 37 °C; pH 6.2). Release ratios are expressed as the mean ± SD ($n = 3$).

from the nanoparticles. There was a dramatic reduction in EGCG release after 24 h, and further release of EGCG required the swelling and degradation of the compact CS–CPP nanoparticles.

CAA of Nanoencapsulated EGCG and Free EGCG. CAA values of nanoencapsulated EGCG and free EGCG generated from the data determined from DCF fluorescence of the cell culture treated with EGCG-loaded CS–CPP nanoparticles and free EGCG, respectively, are shown in Figure 4. The CAA values of nanoencapsulated EGCG were compared to those of free EGCG at the same concentrations, at which the CAA value of vain CS–CPP nanoparticles used for encapsulation was subtracted. It can be seen from Figure 4 that, after encapsulation with the CS–CPP nanoparticles, the CAA value of EGCG increased significantly ($p < 0.01$) compared to that of free EGCG at the same concentration. Nanoencapsulated EGCG exhibited a higher CAA value than free EGCG, suggesting that CS–CPP nanoparticles serve as an ideal delivery system for EGCG and other water-soluble but low cellular permeable bioactive compounds.

Median effect plots for inhibition of peroxy radical-induced DCFH oxidation by the nanoencapsulated EGCG (A) and free EGCG (B) are shown in Figure 5. The value of EC_{50} is the concentration at which $fa/fu = 1$ (i.e., CAA unit = 50). Calculated from the linear regression of the median effect curve, the EC_{50} value for nanoencapsulated EGCG was 12.60

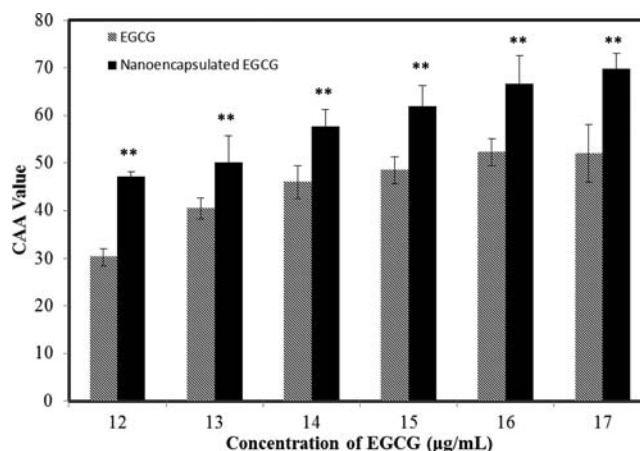


Figure 4. Cellular antioxidant activities of EGCG and nanoencapsulated EGCG with CS–CPP nanoparticles at different EGCG concentrations. Data are presented as the mean ± SD ($n = 6$). (**) Very significant difference ($p < 0.01$; t test).

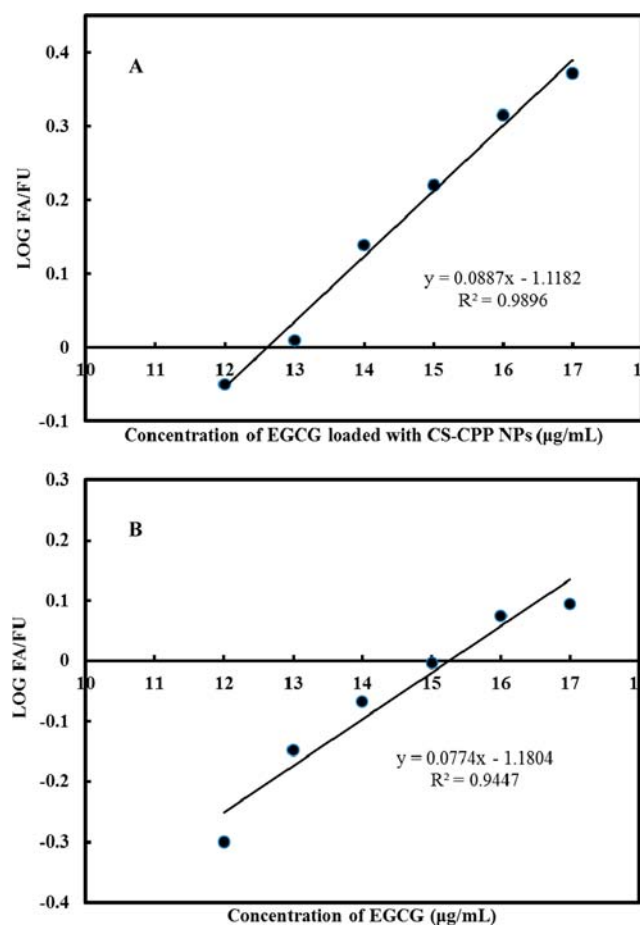


Figure 5. Determination of the EC_{50} of nanoencapsulated EGCG and free EGCG. Median effect plot for inhibition of peroxy radical-induced DCFH oxidation by nanoencapsulated EGCG (A) and free EGCG (B).

$\mu\text{g/mL}$. The EC_{50} value for free EGCG was calculated in the same way to be 15.25 $\mu\text{g/mL}$. Consequently, the EC_{50} of EGCG decreased from 15.25 to 12.60 $\mu\text{g/mL}$ as it was encapsulated with CS–CPP nanoparticles, which also meant improved CAA of EGCG after delivery with the nanoparticles.

Cellular Uptake of Nanoparticles. Cellular uptake studies of FCS and FNPE were performed by visualizing the fluorescence of FITC-labeled CS using fluorescence microscopy. Figure 6 displays the microscopic images of the

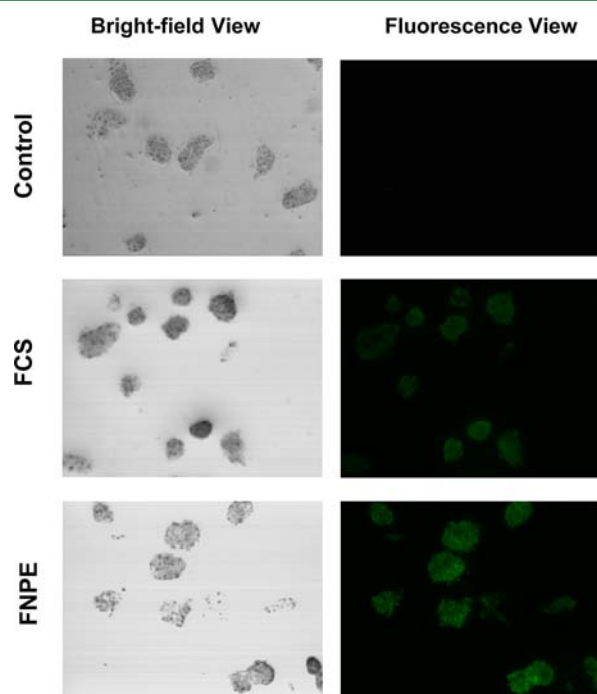


Figure 6. Optical images of HepG2 cells incubated with transport medium (control), FITC-labeled chitosan (FCS), and FITC-labeled CS–CPP nanoparticles loading with EGCG (FNPE), as visualized under an inverted fluorescence microscope.

fluorescence study. Images of control cells without any exposure to drug and cells incubated only with transport medium did not show any fluorescence. However, both the images of the cells incubated with FCS and FNPE (the same incubation time and concentration) showed green fluorescence. Obviously, the fluorescence intensity of the cells treated with FNPE was stronger than that of the cells treated with FCS.

DISCUSSION

A low drug content in the polymeric drug delivery system has been a drawback for the application. In our previous study, the encapsulation efficiency of EGCG in CS–TPP nanoparticles was low (25.8–47.4%) and EGCG was burst-released from the vehicle quickly in the initial 12 h (around 45–60% at 12 h).²⁴ In the present study, we used the reaction between CPP and EGCG that has been confirmed and measured by QCMD in our previous study,¹⁵ to provide the direct drive for entrapping EGCG within CS–CPP nanoparticles. The pH of the medium was fixed at pH 6.2 to mimic the acidic microenvironment in the small intestine. The EGCG-loaded CS–CPP nanoparticles remained intact in the range of pH 2.5–7.0,¹⁵ mimicking the pH environment for oral delivery. The encapsulation efficiency of EGCG with CS–CPP nanoparticles (70.5–81.7%) was about 100% higher than that with the CS–TPP nanoparticle (25.8–47.4%). In comparison to the release profile of EGCG in CS–TPP nanoparticles (around 45–60% at 12 h), the burst release of EGCG in CS–CPP nanoparticles (around 23–40% at 12 h) was slowed in a much more controllable manner. It might be attributed to the binding between EGCG and the

peptides. In addition, a high cross-linking degree between CS and CPP decreased mesh sizes within the nanostructures,¹⁴ which could hinder the burst release of EGCG from the nanoparticles. Considering both the results of encapsulation efficiency and release profile, it can be found that the release rate varied according to different encapsulation efficiencies. The release rate is usually drug-concentration-gradient-driven. A high quantity of loaded-EGCG nanoparticles led to a wide concentration gap between CS–CPP nanoparticles and the release medium, resulting in a high release rate. The combined results of the encapsulation efficiency and controlled release profile of EGCG indicated that the CS–CPP nanoparticle delivery system had certainly overcome the shortcomings of the CS–TPP nanoparticles for the delivery of small molecular drugs, which was suitable for controlling the release of EGCG.

High encapsulation efficiency and low burst release rate of EGCG in CS–CPP nanoparticles were achieved because of the binding between EGCG and CPP. However, it is well-known that the association of polyphenols with proteins forming soluble and insoluble complexes can lead to various unfavorable consequences, resulting in impairment of polyphenol absorption and reduction of health-promotion potential. Therefore, we examined the antioxidant activity of nanoencapsulated EGCG using the CAA assay, which is relatively fast and cost-effective and addresses some issues of uptake, distribution, and metabolism.

The CAA value of EGCG was increased significantly ($p < 0.01$) after delivery with CS–CPP nanoparticles, indicating enhanced bioavailability of EGCG as nanochemoprevention. The CAA value of EGCG was mainly related to its stability, cellular uptake, and metabolites as it was incubated with the HepG2 cells. Consisting of a *meta*-5,7-dihydroxyl-substituted A ring and trihydroxy phenol structures on both the B and D rings, EGCG is a strong antioxidant and is easily auto-oxidized under alkaline or even neutral conditions. It has been reported that EGCG was unstable in McCoy's 5A culture media, with a half-life of less than 30 min, but the half-life of EGCG increased to 130 min in the presence of HT-29 human colon adenocarcinoma cells.²⁹ The retained EGCG was mainly passively diffused into the cells, and it was rapidly biotransformed to its glucuronidated and methylated products in the cell, such as EGCG 4''-glucuronide and 4''-methyl EGCG. These metabolites were then pumped out by multidrug resistance proteins (MRPs). Therefore, auto-oxidization, biotransformation of EGCG, as well as the final pumping out of the metabolites could result in the decrease of the antioxidant activity of EGCG.

The cellular uptake of FCS and FNPE at a non-cytotoxicity CS concentration¹⁵ was examined. We found that both FCS and FNPE could enter the HepG2 cancer cells. Interestingly, the CS–CPP nanoparticles showed an enhanced distribution in the whole cells compared to the parent CS polymers. As the reason, it might be due to the fact that the irregular shape and random structure of CS could deter its entry into the cancer cells.³⁰ In addition, similar results have been reported in early studies.^{31,32} Therefore, CS–CPP nanoparticles were capable of delivery of EGCG into cancer cells for killing the cancer cells.

The elevation of the CAA value of EGCG after encapsulation with CS–CPP nanoparticles can be understood from the protective effect of nanoparticles against the drawbacks of EGCG itself incubated with cells (Figure 7). First, it has been confirmed that the encapsulation of EGCG with CS nanoparticles can stabilize EGCG in an alkaline environment the

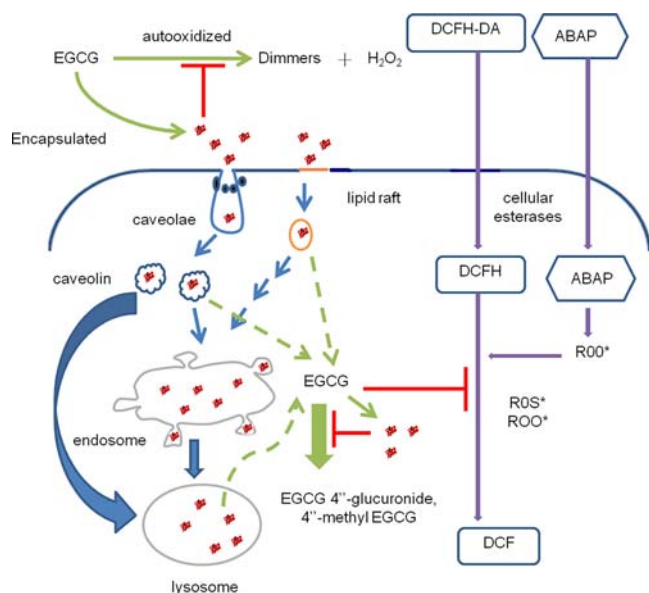


Figure 7. Schematic illustrations showing the potential mechanism of the elevation of the CAA of EGCG after delivery by the CS-CPP nanoparticles.

same as that in the cell antioxidant assay, avoiding the autooxidation of EGCG.³³ Then, the cellular uptake of the EGCG-loaded CS-CPP nanoparticles has been confirmed from the results of the fluorescence images of the HepG2 cells incubated with the nanoparticles. To date, the internalization of polymeric nanoparticles into the cells is achieved through cellular pinocytosis.³⁴ Recently, several reports have discussed the pinocytosis of CS nanoparticles into cells by the basic mechanisms: clathrin-mediated endocytosis, caveolae-mediated endocytosis, macropinocytosis, and lipid raft-mediated endocytosis.^{30,35} Among these mechanisms, caveolae-mediated endocytosis and lipid raft-mediated endocytosis have been identified as the dominant mechanisms. After entering into cells, the CS nanoparticles are first intracellularly trafficked to endosomes and, finally, are entrapped in lysosomes.³⁵ The acidic condition within lysosome (around pH 4.5) is helpful for maintaining the stability of EGCG. In the transport processes, CS-CPP nanoparticles might be able to protect the encapsulated EGCG from being metabolized by blocking the contact between EGCG and corresponding glycosylase and methylase. Finally, EGCG was released to scavenge free radicals inside cancer cells as the CS-CPP nanoparticles were digested in lysosome. Certainly, the detailed information about the intracellular stability of EGCG still needs further investigation.

In conclusion, the encapsulation efficiency of EGCG in CS-CPP nanoparticles was considerably higher than that in CS-TPP nanoparticles, and the burst release of EGCG was slowed in a more controllable manner for CS-CPP nanoparticles than CS-TPP nanoparticles. Cellular uptake of EGCG-loaded CS-CPP nanoparticles was confirmed by green fluorescence inside the HepG2 cells. CAA of EGCG increased significantly after encapsulation in CS-CPP nanoparticles. All of these results suggested that the nanoparticles assembled with bioactive polysaccharide and bioactive peptides should be efficient carriers for enhancing the bioavailability of EGCG.

AUTHOR INFORMATION

Corresponding Author

*Telephone: +86-25-84396791 (X.Z.); 732-932-7193 (Q.H.).
E-mail: zengxx@njau.edu.cn (X.Z.); qhuang@aesop.rutgers.edu (Q.H.).

Funding

This work was supported by The Natural Science Foundation of Jiangsu Province, China (BK2012367), a Young Independent Innovation Fund from Nanjing Agricultural University (Y0201200238), the United States Department of Agriculture National Research Initiative (2009-35603-05071, to Qingrong Huang), and a Project Funded by the Priority Academic Program Development of Jiangsu Higher Education Institutions.

Notes

The authors declare no competing financial interest.

REFERENCES

- (1) Surh, Y. J. Cancer chemoprevention with dietary phytochemicals. *Nat. Rev. Cancer* **2003**, *3*, 768–780.
- (2) Yang, C. S.; Wang, X.; Lu, G.; Picinich, S. C. Cancer prevention by tea: Animal studies, molecular mechanisms and human relevance. *Nat. Rev. Cancer* **2009**, *9*, 429–439.
- (3) Tammela, P.; Ekokoski, E.; Garcia-Horsman, A.; Talman, V.; Finel, M.; Tuominen, R.; Vuorela, P. Screening of natural compounds and their derivatives as potential protein kinase C inhibitors. *Drug Dev. Res.* **2004**, *63*, 76–87.
- (4) Singh, B. N.; Shankar, S.; Srivastava, R. K. Green tea catechin, epigallocatechin-3-gallate (EGCG): Mechanisms, perspectives and clinical applications. *Biochem. Pharmacol.* **2011**, *82*, 1807–1821.
- (5) Chow, H. H. S.; Cai, Y.; Hakim, I. A.; Crowell, J. A.; Shahi, F.; Brooks, C. A.; Dorr, R. T.; Hara, Y.; Alberts, D. S. Pharmacokinetics and safety of green tea polyphenols after multiple-dose administration of epigallocatechin gallate and polyphenon E in healthy individuals. *Clin. Cancer Res.* **2003**, *9*, 3312–3319.
- (6) Lambert, J. D.; Sang, S. M.; Yang, C. S. Biotransformation of green tea polyphenols and the biological activities of those metabolites. *Mol. Pharmacol.* **2007**, *4*, 819–825.
- (7) Leonarduzzi, G.; Testa, G.; Sottero, B.; Gamba, P.; Poli, G. Design and development of nanovehicle-based delivery systems for preventive or therapeutic supplementation with flavonoids. *Curr. Med. Chem.* **2010**, *17*, 74–95.
- (8) Ratnam, D. V.; Ankola, D. D.; Bhardwaj, V.; Sahana, D. K.; Kumar, M. Role of antioxidants in prophylaxis and therapy: A pharmaceutical perspective. *J. Controlled Release* **2006**, *113*, 189–207.
- (9) Siddiqui, I. A.; Adhami, V. M.; Bharali, D. J.; Hafeez, B. B.; Asim, M.; Khwaja, S. I.; Ahmad, N.; Cui, H. D.; Mousa, S. A.; Mukhtar, H. Introducing nanochemoprevention as a novel approach for cancer control: Proof of principle with green tea polyphenol epigallocatechin-3-gallate. *Cancer Res.* **2009**, *69*, 1712–1716.
- (10) Shutava, T. G.; Balkundi, S. S.; Vangala, P.; Steffan, J. J.; Bigelow, R. L.; Cardelli, J. A.; O'Neal, D. P.; Lvov, Y. M. Layer-by-layer-coated gelatin nanoparticles as a vehicle for delivery of natural polyphenols. *ACS Nano* **2009**, *3*, 1877–1885.
- (11) Siddiqui, I. A.; Adhami, V. M.; Ahmad, N.; Mukhtar, H. Nanochemoprevention: Sustained release of bioactive food components for cancer prevention. *Nutr. Cancer* **2010**, *62*, 883–890.
- (12) Siddiqui, I. A.; Mukhtar, H. Nanochemoprevention by bioactive food components: A perspective. *Pharm. Res.* **2010**, *27*, 1054–1060.
- (13) Acosta, E. Bioavailability of nanoparticles in nutrient and nutraceutical delivery. *Curr. Opin. Colloid Interface Sci.* **2009**, *14*, 3–15.
- (14) Hu, B.; Wang, S. S.; Li, J.; Zeng, X.; Huang, Q. R. Assembly of bioactive peptides and chitosan nanocomplexes. *J. Phys. Chem. B* **2011**, *115*, 7515–7523.
- (15) Hu, B.; Ting, Y. W.; Yang, X. Q.; Tang, W. P.; Zeng, X.; Huang, Q. R. Nanochemoprevention from encapsulation of (–)-epigallo-

techin-3-gallate with bioactive peptides/chitosan nanoparticles for enhancing its bioavailability. *Chem. Commun.* **2012**, *48*, 2421–2423.

(16) Hu, B.; Ting, Y. W.; Zeng, X.; Huang, Q. R. Cellular uptake and cytotoxicity of chitosan–caseinophosphopeptides nanocomplexes loaded with epigallocatechin gallate. *Carbohydr. Polym.* **2012**, *89*, 362–370.

(17) Li, B.; Du, W. K.; Jin, J. C.; Du, Q. Z. Preservation of (–)-epigallocatechin-3-gallate antioxidant properties loaded in heat treated β -lactoglobulin nanoparticles. *J. Agric. Food Chem.* **2012**, *60*, 3477–3484.

(18) Peres, I.; Rocha, S.; Gomes, J.; Morais, S.; Pereira, M. C.; Coelho, M. Preservation of catechin antioxidant properties loaded in carbohydrate nanoparticles. *Carbohydr. Polym.* **2011**, *86*, 147–153.

(19) Chen, F.; Shi, Z. L.; Neoh, K. G.; Kang, E. T. Antioxidant and antibacterial activities of eugenol and carvacrol-grafted chitosan nanoparticles. *Biotechnol. Bioeng.* **2009**, *104*, 30–39.

(20) Lee, J. S.; Kim, G. H.; Lee, H. G. Characteristics and antioxidant activity of *Elsholtzia splendens* extract-loaded nanoparticles. *J. Agric. Food Chem.* **2010**, *58*, 3316–3321.

(21) Wolfe, K. L.; Liu, R. H. Cellular antioxidant activity (CAA) assay for assessing antioxidants, foods, and dietary supplements. *J. Agric. Food Chem.* **2007**, *55*, 8896–8907.

(22) Yu, H. L.; Li, J.; Shi, K.; Huang, Q. R. Elevated cellular antioxidant activity of curcuminoids encapsulated in modified epsilon polylysine micelles. *Food Funct.* **2011**, *2*, 373–380.

(23) Sessa, M.; Tsao, R.; Liu, R. H.; Ferrari, G.; Donsi, F. Evaluation of the stability and antioxidant activity of nanoencapsulated resveratrol during in vitro digestion. *J. Agric. Food Chem.* **2011**, *59*, 12352–12360.

(24) Hu, B.; Pan, C. L.; Sun, Y.; Hou, Z. Y.; Ye, H.; Hu, B.; Zeng, X. Optimization of fabrication parameters to produce chitosan–tripolyphosphate nanoparticles for delivery of tea catechins. *J. Agric. Food Chem.* **2008**, *56*, 7451–7458.

(25) Hu, B.; Wang, L.; Zhou, B.; Zhang, X.; Sun, Y.; Ye, H.; Zhao, L. Y.; Hu, Q. H.; Wang, G. X.; Zeng, X. Efficient procedure for isolating methylated catechins from green tea and effective simultaneous analysis of ten catechins, three purine alkaloids, and gallic acid in tea by high-performance liquid chromatography with diode array detection. *J. Chromatogr., A* **2009**, *1216*, 3223–3231.

(26) Huang, M.; Khor, E.; Lim, L. Y. Uptake and cytotoxicity of chitosan molecules and nanoparticles: Effects of molecular weight and degree of deacetylation. *Pharm. Res.* **2004**, *21*, 344–353.

(27) Bodnar, M.; Hartmann, J. F.; Borbely, J. Preparation and characterization of chitosan-based nanoparticles. *Biomacromolecules* **2005**, *6*, 2521–2527.

(28) Bodnar, M.; Hartmann, J. F.; Borbely, J. Synthesis and study of cross-linked chitosan-*N*-poly(ethylene glycol) nanoparticles. *Biomacromolecules* **2006**, *7*, 3030–3036.

(29) Hong, J.; Lu, H.; Meng, X. F.; Ryu, J. H.; Hara, Y.; Yang, C. S. Stability, cellular uptake, biotransformation, and efflux of tea polyphenol (–)-epigallocatechin-3-gallate in HT-29 human colon adenocarcinoma cells. *Cancer Res.* **2002**, *62*, 7241–7246.

(30) Nam, H. Y.; Kwon, S. M.; Chung, H.; Lee, S. Y.; Kwon, S. H.; Jeon, H.; Kim, Y.; Park, J. H.; Kim, J.; Her, S.; Oh, Y. K.; Kwon, I. C.; Kim, K.; Jeong, S. Y. Cellular uptake mechanism and intracellular fate of hydrophobically modified glycol chitosan nanoparticles. *J. Controlled Release* **2009**, *135*, 259–267.

(31) Jia, X. Y.; Chen, X.; Xu, Y. L.; Han, X. Y.; Xu, Z. R. Tracing transport of chitosan nanoparticles and molecules in Caco-2 cells by fluorescent labeling. *Carbohydr. Polym.* **2009**, *78*, 323–329.

(32) Loh, J. W.; Yeoh, G.; Saunders, M.; Lim, L. Y. Uptake and cytotoxicity of chitosan nanoparticles in human liver cells. *Toxicol. Appl. Pharmacol.* **2010**, *249*, 148–157.

(33) Dube, A.; Ng, K.; Nicolazzo, J. A.; Larson, I. Effective use of reducing agents and nanoparticle encapsulation in stabilizing catechins in alkaline solution. *Food Chem.* **2010**, *122*, 662–667.

(34) Conner, S. D.; Schmid, S. L. Regulated portals of entry into the cell. *Nature* **2003**, *422*, 37–44.

(35) Chiu, Y. L.; Ho, Y. C.; Chen, Y. M.; Peng, S. F.; Ke, C. J.; Chen, K. J.; Mi, F. L.; Sung, H. W. The characteristics, cellular uptake and

intracellular trafficking of nanoparticles made of hydrophobically-modified chitosan. *J. Controlled Release* **2010**, *146*, 152–159.